Published in final edited form as:

*ACS Chem Biol*. 2017 April 21; 12(4): 1038–1046. doi:10.1021/acschembio.6b01040.

# Eg5 inhibitors have contrasting effects on microtubule stability and metaphase spindle integrity

**Geng-Yuan Chen**[1], **You Jung Kang**[1], **A. Sophia Gayek**[2], **Wiphu Youyen**[3], **Erkan Tüzel**[3], **Ryoma Ohi**[2], and **William O. Hancock**[1,*]

[1]Department of Biomedical Engineering, Pennsylvania State University, University Park, PA 16802

[2]Department of Cell and Developmental Biology, Vanderbilt University, Nashville, TN 37203

[3]Department of Physics, Worcester Polytechnic Institute, Worcester, MA 01609

## Abstract

To uncover their contrasting mechanisms, antimitotic drugs that inhibit Eg5 (kinesin-5) were analyzed in mixed-motor gliding assays of kinesin-1 and Eg5 motors in which Eg5 "braking" dominates motility. Loop-5 inhibitors (monastrol, STLC, ispinesib and filanesib) increased gliding speeds, consistent with inducing a weak-binding state in Eg5, whereas BRD9876 slowed gliding, consistent with locking Eg5 in a rigor state. Biochemical and single-molecule assays demonstrated that BRD9876 acts as an ATP- and ADP-competitive inhibitor with 4 nM $K_I$. Consistent with its microtubule polymerase activity, Eg5 was shown to stabilize microtubules against depolymerization. This stabilization activity was eliminated in monastrol, but was enhanced by BRD9876. Finally, in metaphase-arrested RPE-1 cells, STLC promoted spindle collapse, whereas BRD9876 did not. Thus, different Eg5 inhibitors impact spindle assembly and architecture through contrasting mechanisms, and rigor inhibitors may paradoxically have the capacity to stabilize microtubule arrays in cells.

### Keywords

kinesin; microtubule; single-molecule imaging; molecular motor; mitotic spindle; drug screening; chemical kinetics

Homotetrameric kinesin-5 Eg5/KSP motors are best known for their capacity to slide antiparallel microtubules apart during spindle formation[1,2] and neurogenesis[3,4]. By acting as the dominant MT sliding factor during cell division, Eg5 limits the maximum speed of microtubule (MT) sliding during both spindle assembly[5] and midzone elongation[6,7]. On

*To whom correspondence should be addressed: William O. Hancock, Department of Biomedical Engineering, Penn State University, 205 Hallowell Building, University Park, PA, USA, Tel.: (814) 863-0492; Fax: (814) 863-0492; wohbio@engr.psu.edu.

**AUTHOR CONTRIBUTIONS**

G.-Y.C and W.O.H designed the study. Y.J.K. acquired and analyzed the mixed-motor gliding assays and stopped-flow measurements. A.S.G. and R.O. carried out cell experiments. W.Y. and E.T. carried out computational simulations. G.-Y.C., W.O.H, R.O. and E.T. wrote the manuscript. All authors reviewed the results, and approved the final version of the manuscript.

**COMPETING INTERESTS**

The listed authors declare that they have no conflicts of interest with the contents of this article.

parallel MTs, kinesin-5 motors act as passive cross-linkers, a non-motile function that has been suggested to stabilize spindle architecture through bundling of MTs near the spindle pole[8]. In addition to these mechanical functions, we recently showed that Eg5 pauses at MT plus-ends, where the motor increases the growth rate and reduces the catastrophe frequency of dynamic MTs, likely due to stabilizing of incoming tubulin dimers at the plus-end[9]. This MT-polymerase activity is hypothesized to enhance the *in vivo* function of Eg5 by increasing the degree of astral and midzone MT overlap and by contributing to metaphase MT flux[10].

Eg5 has several mechanistic features that distinguish it from kinesin-1 (KHC or conventional kinesin), and may help to explain its diverse physiological functions. Engineered Eg5 dimers have a large stall force, and display minimal processivity[11], consistent with Eg5 working in teams during spindle formation[2,12]. Additionally, Eg5 walks with a 10-fold slower velocity than kinesin-1[11,13,14], and it is able to resist large mechanical loads (~10 pN) in either the plus- or minus-end directions[15–17], which contrasts with the directional dependence of kinesin-1[18]. These properties likely result, at least in part, from the motor spending most of its ATP hydrolysis cycle in a state in which both heads are bound to the microtubule (two-head-bound state), a property not shared by kinesin-1[11,14].

Due to its crucial functions in mitosis, Eg5 is a major target for anti-proliferative chemotherapeutic agents[19]. Several inhibitors have been identified that bind at or near loop L5, stabilize the bound nucleotide and trap the motor in a weak-binding state[20–24]. These ATP-uncompetitive inhibitors include pyrimidine derivatives (monastrol[25,26]), quinazolinone (ispinesib[27]), thiadiazoles (filanesib[28], litronesib[29], K858[30]), and S-trityl-L-cysteine (STLC)[22]. Several compounds that that generate rigor-like states in Eg5 have also been documented. The thiazole FCPT[31,32] is thought to act as an ATP competitive inhibitor by binding directly to the nucleotide binding site. In contrast, mutagenesis and structural analysis revealed that biaryl compounds GSK-1[33], PVZB1194[34,35] act as ATP-competitive inhibitors but bind near the α4–α6 interface[33,35,36]; thus they behave as allosteric competitive inhibitors of ATP binding. A related compound, BRD9876, was recently identified as an Eg5 inhibitor that binds to the α4–α6 interface, but was reported to be ATP non-competitive, and to preferentially bind to MT-bound Eg5[36]. Because of their different modes of action, these inhibitors may have different effects on the ability of Eg5 to stabilize MTs against depolymerization. The polymerase activity was only recently reported[9], and inhibitors may provide chemical probes for understanding the Eg5 polymerase mechanism and modulating its activity in cells.

We began from a mechanically-based drug-screening method to classify inhibitors by their effects on the “braking” ability of Eg5 in mixed-motor microtubule gliding assays. “L5 inhibitors” including monastrol, ispinesib, STLC and filanesib (ARRY-520) reduced Eg5’s braking ability, whereas the “rigor inhibitor” BRD9876 enhanced the braking ability of Eg5. Detailed investigations revealed that different classes of compounds have distinct effects on MT stability and spindle integrity: L5 inhibitors abolish the ability of Eg5 to stabilize MTs against depolymerization and cause metaphase spindle collapse, whereas the rigor inhibitor BRD9876 stabilizes MTs against depolymerization *in vitro* and stabilizes metaphase spindles against collapse. This work extends our understanding of how Eg5 motors modulate

MT dynamics and delineate contrasting strategies for achieving mitotic arrest by targeting Eg5.

## RESULTS AND DISCUSSION

### Loop-5 inhibitors reduce and rigor inhibitors enhance the “braking” ability of Eg5

Mixed motor gliding assays provide a mean to assess the mechanical performance of motors, and hence provide a potential platform for screening small-molecule compounds that mechanically modulate Eg5 (Figure 1a,b)[15,20,37]. As seen in Figure 1c, uniform populations of KHC moved MT at ~700 nm/s[18], uniform populations of Eg5 moved MT at ~70 nm/s[14], and a minor fraction of Eg5 (22%) was sufficient to slow velocity to the Eg5 speed, consistent with this motor’s documented “braking” ability[12,15,20,38]. In 100 μM STLC, the MT gliding activity of Eg5 was abolished at high fractions of Eg5, consistent with full motor inhibition. At intermediate Eg5 densities, gliding velocities in STLC significantly increased, demonstrating that STLC strongly diminishes the braking ability of Eg5 (Figure 1c). To test whether different Loop-5 inhibitors generated equivalent mechanical states of Eg5, experiments were repeated with monastrol, ispinesib and filanesib (ARRY-520) (Figure 1d). The results were qualitatively similar, but analysis of the velocity at 22% Eg5 indicates that the degree of mechanical inhibition varied, following the sequence STLC = filanesib > ispinesib = monastrol (Figure 1d).

The recently reported naphthalene compound BRD9876[36] behaved differently from the Loop-5 inhibitors. In 100 μM BRD9876, the MT gliding velocity was reduced from control at all mol fractions of Eg5 (Figure 1c,d). The steep fall in velocity with small proportions of Eg5 indicates that BRD9876 enhances the “braking” ability of Eg5, consistent with BRD9876-inhibited motors being in a strong-binding state. Based on this contrasting mechanical response, BRD9876 was classified as a “rigor” Eg5 inhibitor, similar to other reported rigor inhibitors[31–35].

To better understand the different modes of inhibition, we analyzed gliding velocities using a recently developed model that recapitulates mixed-motor gliding based on the velocities and force-dependent off-rates of the relevant motors[15]. The kinesin-1 mechanical parameters and the unloaded velocities of both motors are experimentally constrained[18], leaving the force-dependent detachment rate of Eg5, $k_{off}(F) = k_{off}^{0} * e^{F/Fc}$ the only unknown. The unloaded detachment rate, $k_{off}^{0}$, was measured by single-molecule TIRF microscopy (Figure S1), and the critical detachment force, $F_c$, was determined by iterative fitting of the model to the experiments (Figure S2). Interestingly, while all of the L5 inhibitors increased the unloaded off-rate, they can be separated into two groups: a) the less-potent monastrol and ispinesib, which have larger $F_c$ than the control, meaning that the resistance of Eg5 detachment to load is maintained, and b) the more potent STLC and filanesib, which have much smaller $F_c$ than the control, meaning that motor detachment is strongly dependent on load. This functional assay revealed differences in the potency of different L5 inhibitors that from crystallography studies have been shown to have only minimal structural differences[19]. Finally, BRD9876 had a very slow unloaded off-rate and a similar $F_c$ as the control, consistent with the motor being in a strong-binding state that resists detachment by load. Thus, the velocities in Figure

1d can be quantitatively explained by specific effects of different inhibitors on $k_{off}^0$ and $F_c$. The results are summarized in Table 1.

## Drugs produce contrasting effects on the diffusion of Eg5 along microtubules

To further investigate the different modes of Eg5 inhibition, single-molecule tracking measurements of Qdot655-labeled Eg5 were carried out in 5 mM ATP (Figure 2a) or 5 mM ADP (Figure 2b). Traces where motors dwelled for more than 1 second (20 frames) were collected, and a 1D Gaussian function was fit to each row of the kymograph to obtain the center positions. To analyze the mean-square displacement (MSD), either a quadratic form ($MSD(\Delta t) = v^2\Delta t^2 + 2D\Delta t + \sigma^2$) or a linear form ($MSD(\Delta t) = 2D\Delta t + \sigma^2$) was assigned based on the presence or the absence of stepping. In saturating ATP, the motor had a velocity of 66 ± 26 nm/s and a negligible diffusion coefficient of 594 ± 167 $nm^2/s$, consistent with our previous findings that Eg5 dimers step processively in ATP[14]. In contrast, in saturating ADP the motor diffused along the microtubule with $D$ = 3,845 ± 119 $nm^2/s$. We used this value as a benchmark for Eg5 in a weak-binding state.

Although both classes of drugs completely blocked directional movement (Figure 1), different inhibitors had contrasting effects on the diffusive properties of Eg5. Treatment with STLC resulted in motors diffusing along MTs relatively freely, with $D$ = 2,467 ± 161 $nm^2/s$ in saturating ATP and $D$ = 4,182 ± 116 $nm^2/s$ in saturating ADP (Figure 2). These results are consistent with previous work that found that STLC blocks ADP release and the weak-to-strong transition[23,24]. Further support for this mechanism comes from the similarity in the diffusion constant in ADP in the presence and absence of STLC (Figure 2). Using stopped-flow, we confirmed that STLC and other L5 inhibitors slow the Eg5 MT-stimulated mADP release by greater than 20-fold (Figure S3) and we also observed that STLC and filanesib, which had the strongest mechanical inhibition in the mixed motor gliding assay (Figure 1d) most strongly inhibited the MT-stimulated mADP release rate. The finding that STLC leads to a higher diffusion constant in ADP than in ATP can be interpreted either that the STLC-mediated diffusion in ATP occurs in the ADP-Pi state[14] or that STLC-inhibited Eg5 spends approximately half of its cycle in a high affinity state in ATP.

In marked contrast, BRD9876 caused Eg5 to bind tightly to MTs in either ATP ($D$ = 200 ± 25 $nm^2/s$) or ADP ($D$ = 75 ± 37 $nm^2/s$), with the long dwell times consistent with BRD9876 trapping the motor in a strong-binding state. Based on the MT gliding and single-molecule diffusion results, BRD9876 could inhibit Eg5 by: 1) trapping the motor in an apo state due to interfering with nucleotide exchange, 2) blocking hydrolysis so that the motor is trapped in an ATP state, or 3) causing a structural change that enhances MT binding independent of the nucleotide state of the motor. In the next set of experiments, we set out to test these different potential mechanisms.

## BRD9876 generates an apo-state Eg5

To better understand the mechanism of Eg5 inhibition by BRD9876 we performed microtubule-stimulated ATPase assays at varying ATP and MT concentrations. When ATP concentration is varied, an ATP non-competitive inhibitor is predicted to change the $V_{max}$ without a change in $K_M^{ATP}$, whereas an ATP competitive inhibitor should change $K_M^{ATP}$

with no alteration in $V_{max}$. As seen in Figure 3a, increasing concentrations of BRD9876 increased the $K_M^{ATP}$ but had negligible effect on the $V_{max}$, consistent with the drug being a competitive inhibitor of ATP binding with a $K_I$ of 3.8 ± 1.5 nM (see also Figure S4). This result differs from previous work showing that BRD9876 is an ATP-noncompetitive inhibitor of Eg5[36], but it is consistent with biochemical results from other inhibitors that bind at the α4–α6 interface[31–35]. Molecular docking simulations of BRD9876 binding to apo-Eg5 predicted that BRD9876 binds at the same site on Eg5 as another well-characterized rigor inhibitor PVZB1194 (Figure S5), consistent with the mutagenesis prediction[36]. Thus, we conclude that in ATP, BRD9876 induces an apo-state of Eg5 and this strong-binding state underlies the motor's strong resistance against assisting loads (Figure 1) and lack of single-molecule diffusion (Figure 2) in the presence of this inhibitor. To test for changes in the apparent MT affinity, the MT-dependence of the ATPase activity was examined at 3 mM ATP and increasing drug concentrations (Figure 3b). Based on the similarity of slopes, BRD9876 decreased the $K_M^{MT}$ and $V_{max}$ to the same degree, indicating MT-uncompetitive inhibition. This result indicates that MT-binding is required for drug binding (Figure 3b diagram), which may be due to the high ADP affinity of Eg5 in solution[39].

Because BRD9876 also inhibits diffusion of Eg5 in 5 mM ADP (Figure 2), we hypothesized that BRD9876 may also be a competitive inhibitor of ADP. To test whether the BRD9876-inhibited Eg5 is able to exchange ADP, we used single-molecule TIRF to measure the duration of dimeric Eg5-MT binding events at varying ADP concentrations in the presence and absence of drug (Figure 3c). At limiting ADP concentrations the MT unbinding rate is near zero (confirming that the apo-state binds tightly), and at saturating ADP concentrations the MT unbinding rate plateaus; the ADP concentration at which the rate is half-maximal represents the $K_D$ for ADP binding to the Eg5-MT species[40] (see Figure 3c inset). Under control conditions, Eg5 had a maximal MT-unbinding rate of 0.55 ± 0.02 $s^{-1}$ and an ADP affinity of $K_D^{ADP}$ = 86 ± 7 μM ADP (Figure 3c), in agreement with previous work[14]. In the presence of BRD9876, the effective nucleotide affinity dropped 25-fold ($K_D^{apparent}$ = 2.2 ± 1.1 mM ADP), while the maximal off-rate remained at 0.52 ± 0.18 $s^{-1}$ (Figure 3c). The lack of effect on the maximal off-rate is consistent with BRD9876 acting purely as a nucleotide binding inhibitor rather than causing a structural change in the Eg5-MT interface. The ~25-fold shift in the apparent $K_D^{ADP}$ in the presence of 100 nM BRD9876 is consistent with the drug having a $K_I$ of 4.1 nM, which closely matches the $K_I$ of 3.8 ± 1.5 nM from the ATPase assays (Figure 3a and Figure S4). These competitive inhibition results using two independent assays are consistent with a model in which binding of BRD9876 disrupts the nucleotide-binding pocket to exclude both ATP and ADP, thereby generating a strong-binding apo-state species.

## BRD9876 enhances Eg5-mediated MT-stabilization

Eg5 was recently shown to possess MT polymerase activity through a mechanism that is thought to involve stabilization of incoming tubulin into the MT lattice[9]. One prediction from this model is that Eg5 inhibitors that weaken Eg5-MT interactions should reduce the MT stabilization activity, whereas inhibitors that strengthen Eg5-MT interactions may enhance the motors' microtubule stabilization activity. To test this prediction, we bound

Cy5-labeled taxol-stabilized MTs to coverslip surfaces, washed out taxol to induce MT depolymerization, and measured the MT-shortening rate under different conditions (Figure 4a). Under control conditions (which included 1 vol% DMSO) MT shrank at an average rate of 4.2 ± 0.2 nm/s; (mean ± s.e.m., N = 36). When Eg5 was introduced in the presence of 5 mM ATP, the shortening rate was reduced to 2.9 ± 0.1 nm/s (N = 48), demonstrating the MT stabilization activity of active Eg5. In the presence of monastrol, the shortening rate returned to the control (MON: 4.5 ± 0.2 nm/s, N = 20), confirming that inhibitors that weaken the Eg5 binding eliminate its MT stabilization properties. In contrast, in the presence of BRD9876 the shortening rate fell to near zero (BRD: 0.7 ± 0.1 nm/s, N = 79). As a positive control, enhancing Eg5-MT binding by replacing ATP with AMPPNP or no nucleotide also led to strong stabilization of the MT against depolymerization (AMPPNP: 0.3 ± 0.1 nm/s, N = 33; Apo-state: 1.2 ± 0.1 nm/s, N = 25). Therefore, although BRD9876 inhibits the motor's ability to step along the microtubule, by inducing a strongly-bound state the drug actually enhances the motors ability to stabilize MTs against depolymerization.

## BRD9876 does not induce metaphase spindle collapse

In dividing cells, Eg5 activity is important during prometaphase for separating duplicated centrosomes, and during metaphase for generating outward-directed forces that stabilize the mitotic spindle[25,41]. Eg5 inhibitors that induce either weak- or strong-binding states have been shown to inhibit spindle formation, but they are predicted to have contrasting effects on spindles that have already formed – inhibitors that generate weak-binding states should cause spindle collapse, whereas inhibitors that generate strong binding state should not. To test whether different drugs have different effects on metaphase spindle integrity, we arrested RPE-1 cells in metaphase using 5 μM of the proteasome inhibitor MG-132 for 90 minutes, followed by exposing cell lines to either a L5 inhibitor (STLC[41]) or rigor inhibitor (BRD9876) for another 90 minutes, and then measured the degree of monopolarity (Figure 4b). In control cells (MG-132 only), spindles were uniformly bipolar, consistent with metaphase arrest. STLC treatment produced a monopolarity index of 69 ± 9% cells being monopolar, consistent with weak-binding motors being unable to resist inward-directed spindle forces[41]. In contrast, in BRD9876-treated cells, only 1 ± 1% of pre-anaphase structures were monopolar, consistent with the notion that BRD9876-induced "rigor" Eg5 that stabilizes the metaphase spindle. Thus, the weak- and strong-binding inhibited states observed *in vitro* are recapitulated in dividing cells, and impact the mitotic spindle differently (Figure S6).

## Differing mechanisms of Eg5 inhibition

We found that small molecule inhibitors can be classified into "Loop-5" inhibitors that all reduce the ability of Eg5 to resist mechanical loads, and "rigor" inhibitors that enhance the ability of Eg5 to resist mechanical loads. Using a phenotypic screening approach, Chattopadhyay *et al.*[36] found that, similar to monastrol[25] and STLC[23], BRD9876 treatment resulted in enhanced spindle monopolarity and G2/M arrest in multiple myeloma 1S cells. Analysis of phospho-mimetic Eg5 mutants in cells was used to argue that BRD9876 preferentially binds to and inhibits MT-bound Eg5, and mutagenesis was used to argue that the compound binds near the junction of helices α4 and α6, similar to other rigor inhibitors[33,34]. In our cell-based assays, we also found that BRD9876 generated monopolar

spindles in dividing RPE-1 cells, and also observed that BRD9876 caused Eg5 to concentrate at the spindle poles (the site of highest microtubule density in the cell), whereas STLC largely knocked Eg5 off the spindle (Figure S6)[41]. This intracellular localization is consistent with our *in vitro* assays demonstrating that BRD9876 induces a strong-binding state whereas STLC induces a weak-binding state in Eg5.

In contrast to Chattopadhyay *et al.*, who concluded from monomeric Eg5 ATPase experiments that BRD9876 acts as an ATP-noncompetitive inhibitor[36], we found that BRD9876 acts as a competitive inhibitor of ATP. To investigate this question further, we measured the microtubule binding durations of dimeric Eg5 in ADP; this assay uses dimeric rather than monomeric motors and focuses solely on nucleotide binding and motor-MT interactions, simplifying the analysis. Again, we found that the data were consistent with competitive inhibition of nucleotide binding, and the $K_I$ of 4.1 nM from the ADP dimer experiments matched the $K_I$ of 3.8 nM from the monomer ATPase experiments, further supporting our claim. Thus, we conclude that BRD9876-inhibited Eg5 is in a MT-bound apo-state, and interpreted the $IC_{50}$ of 2–10 μM measured by Chattopadhyay *et al.* as a $K_I$ in the nM-range in the presence of mM-level of ATP across varying cells (see also Figure S4). This ATP-competitive inhibition is consistent with what was found for the biaryl compounds GSK-1[33] and PVZB1194[34], both of which were shown to dock at the α4/α6 interface (Figure S5)[35]. The inhibitor BI8, which also binds at the α4/α6 interface was reported to act as a mixed ATP-uncompetitive inhibitor of Eg5 ATPase activity[42]. However, the drug was shown to also bind to a site near L5[43], meaning that the effect on $V_{max}$ could be due to the Loop-5 binding site. Hence, those data do not rule out the possibility that BI8 binding to the α4/α6 site acts as an ATP-competitive inhibitor.

The MT-uncompetitive behavior reported for rigor inhibitors[31,33,34] implies that inhibitors only bind to the enzyme-substrate complex (Eg5-MT) but not to the free enzyme (Eg5). It is well established that microtubule binding reduces the Eg5 nucleotide affinity[14,39], and this apparent drug binding selectivity may simply result from free motors having a higher nucleotide affinity – drug binding can outcompete nucleotide binding for MT-bound Eg5 where the nucleotide affinity is reduced, but in solution nucleotide binding to Eg5 outcompetes drug binding. The decrease in nucleotide binding affinity upon microtubule binding has been structurally interpreted in kinesin-1 by the “seesaw” mechanism, in which lateral rotation of a subdomain of the kinesin head alternatively opens the nucleotide binding and neck-linker docking clefts[44]. In kinesin-5, which has a unique L5 latch[45], the coupling between the switch and neck linker domains is diminished and the structural transition are not as sharp as kinesin-1[17,46]. These differences may lead to the slower observed MT-stimulated ADP release in Eg5 compared to kinesin-1[13,14,39]. One possible inhibition mechanism is that in apo-Eg5, binding of rigor inhibitors to the α4/α6 interface may allosterically close the nucleotide cleft, thereby blocking nucleotide exchange[33,35].

## Effects of inhibitors on MT dynamics and spindle stability

Because BRD9876 inhibits motor function, it is surprising that the drug enhances the ability of Eg5 to stabilize MTs. In previous work, we showed that Eg5 dimers enhance the growth rate of dynamic MTs, reduce the catastrophe frequency, and promote the formation of long

(~μm) protofilament curls at growing plus ends[9], which was interpreted by a model in which Eg5 at a growing plus-end uses its head domains to stabilize incoming tubulin. Here we assessed the influence of dimeric Eg5 on the MT shrinkage rate following taxol washout and found that BRD9876-inhibited motors strongly stabilized MTs against depolymerization (Figure 4a and 5), presumably by binding to adjacent tubulin on a protofilament and stabilizing them in the microtubule lattice. The potency of this stabilization is emphasized by the fact that control experiments in ATP were performed at 40 nM motor concentration, whereas the effects of drug inhibition was performed at only 5 nM Eg5 dimer concentration. Also, the stabilization activities in AMPPNP and no nucleotide confirm that neither ATP hydrolysis nor processive walking are required for Eg5-mediated microtubule stabilization. It is interesting to speculate the degree to which the cellular effects of BRD9876 are due to the lack of processive plus-end motility, MT crosslinking by inhibited Eg5, and enhanced stabilization of MTs by inhibited Eg5. One possibility is that BRD9876-inhibited Eg5 has a taxol-like effect in stabilizing microtubules in cells. More detailed cellular investigations will be required to assess the contribution of these different activities to the effect of BRD9876 on dividing cells.

The different inhibition mechanisms of L5 and rigor inhibitors revealed the contribution of Eg5 to both spindle formation and maintenance. Because they both inhibit motor pushing forces, it is not surprising that both inhibitor classes blocked spindle formation. Inhibition following metaphase arrest revealed that inward-directed forces in the spindle are sufficient to collapse the spindle when Eg5 is inhibited in the weak-binding state, but locking Eg5 motors to overlapping microtubules stabilizes the spindle against collapse even though the motor is inhibited. While cell bipolarity was not affected by BRD9876, chromosomal alignment was disrupted (Figure 4b and 5), indicating some mechanical factors beyond Eg5 that regulate spindle geometries and force balance. Previous work showed that application of STLC in HeLa cells arrested in metaphase was not sufficient to induce spindle collapse; most likely this is due to the prominent kinetochore-fibers that must shorten to enable spindle collapse[41]. In contrast, the K-fibers are more dynamic in the RPE-1 cells used here[47]. Recent studies showed that in cells where Eg5 is inhibited by mutation or FCPT treatment, the kinesin-12 motor KIF15 is able to partially replace Eg5 function to achieve spindle assembly[48]. It is possible that in BRD9876-treated cells, KIF15 activity, perhaps activated by Eg5-induced microtubule bundling or crosslinking, is contributing to stabilization of the spindle[49]. The different inhibited states induced by loop-5 and rigor Eg5 inhibitors should provide a chemical probe for dissecting the diverse roles of Eg5 in mitosis.

## Supplementary Material

Refer to Web version on PubMed Central for supplementary material.

## Acknowledgments

The authors gratefully acknowledge D. Arginteanu for assistance in protein purification, R. Chern for the suggestions on molecular docking simulations, Y. Chen for developing the experimental setup of the Eg5 polymerase mechanism, and K. Mickolajczyk for suggestions in MT dynamic instability assays. A portion of the bacterial culture work was carried out at the Penn State Huck Institutes for Life Sciences Fermentation Facility with the assistance of M. Signs. This work was supported by NIH R01 GM076476 to W.O.H., NIH R01 GM100076 to

W.O.H. and E.T., and NIH R01 GM086610 and a career development award from the Leukemia and Lymphoma Society to R.O.

This work was supported by NIH R01 GM076476 to W.O.H, NIH R01 GM100076 to W.O.H. and E.T., NIH R01 GM086610 and a career development award from the Leukemia and Lymphoma Society to R. O.

## The abbreviations used are

| | |
|---|---|
| **mADP** | 2′-(or-3′)-O-(N-Methylanthraniloyl) ADP |
| **MT** | microtubule. BRD, BRD9876 |
| **STLC** | S-trityl-$_L$-cysteine |
| **FCPT** | 2-(1-(4-fluorophenyl)cyclopropyl)-4-(pyridin-4-yl) thiazole |

## References

1. Sawin KE, LeGuellec K, Philippe M, Mitchison TJ. Mitotic spindle organization by a plus-end-directed microtubule motor. Nature. 1992; 359:540–3. [PubMed: 1406972]
2. Kapitein LC, Peterman EJG, Kwok BH, Kim JH, Kapoor TM, Schmidt CF. The bipolar mitotic kinesin Eg5 moves on both microtubules that it crosslinks. Nature. 2005; 435:114–8. [PubMed: 15875026]
3. Nadar VC, Ketschek A, Myers KA, Gallo G, Baas PW. Kinesin-5 is essential for growth-cone turning. Curr Biol. 2008; 18:1972–7. [PubMed: 19084405]
4. Falnikar A, Tole S, Baas PWP, Forscher P. Kinesin-5, a mitotic microtubule-associated motor protein, modulates neuronal migration. Mol Biol Cell. 2011; 22:1561–1574. [PubMed: 21411631]
5. Saunders AM, Powers J, Strome S, Saxton WM. Kinesin-5 acts as a brake in anaphase spindle elongation. Curr Biol. 2007; 17:453–454.
6. Hu CK, Coughlin M, Field CM, Mitchison TJ. KIF4 regulates midzone length during cytokinesis. Curr Biol. 2011; 21:815–824. [PubMed: 21565503]
7. Collins E, Mann BJ, Wadsworth P. Eg5 restricts anaphase B spindle elongation in mammalian cells. Cytoskeleton. 2014; 71:136–144. [PubMed: 24285623]
8. Uteng M, Hentrich C, Miura K, Bieling P, Surrey T. Poleward transport of Eg5 by dynein-dynactin in Xenopus laevis egg extract spindles. J Cell Biol. 2008; 182:715–726. [PubMed: 18710923]
9. Chen Y, Hancock WO. Kinesin-5 is a microtubule polymerase. Nat Commun. 2015; 6:8160. [PubMed: 26437877]
10. Miyamoto DT, Perlman ZE, Burbank KS, Groen AC, Mitchison TJ. The kinesin Eg5 drives poleward microtubule flux in Xenopus laevis egg extract spindles. J Cell Biol. 2004; 167:813–818. [PubMed: 15583027]
11. Valentine MT, Fordyce PM, Krzysiak TC, Gilbert SP, Block SM. Individual dimers of the mitotic kinesin motor Eg5 step processively and support substantial loads in vitro. Nat Cell Biol. 2006; 8:470–6. [PubMed: 16604065]
12. Shimamoto Y, Forth S, Kapoor TM. Measuring Pushing and Braking Forces Generated by Ensembles of Kinesin-5 Crosslinking. Dev Cell. 2015; 34:669–681. [PubMed: 26418296]
13. Mickolajczyk KJ, Deffenbaugh NC, Arroyo JO, Andrecka J, Philipp K, Hancock WO. Kinetics of nucleotide-dependent structural transitions in the kinesin-1 hydrolysis cycle. Proc Natl Acad Sci. 2015:8–11.
14. Chen GY, Mickolajczyk KJ, Hancock WO. The Kinesin-5 Chemomechanical Cycle is Dominated by a Two-heads-bound State. J Biol Chem. 2016; 291:20283–20294. [PubMed: 27402829]
15. Arpağ G, Shastry S, Hancock WO, Tüzel E. Transport by populations of fast and slow kinesins uncovers novel family-dependent motor characteristics important for in vivo function. Biophys J. 2014; 107:1896–1904. [PubMed: 25418170]

16. Valentine MT, Block SM. Force and premature binding of ADP can regulate the processivity of individual Eg5 dimers. Biophys J. 2009; 97:1671–1677. [PubMed: 19751672]
17. Muretta JM, Jun Y, Gross SP, Major J, Thomas DD, Rosenfeld SS. The structural kinetics of switch-1 and the neck linker explain the functions of kinesin-1 and Eg5. Proc Natl Acad Sci. 2015; 112:E6606–13. [PubMed: 26627252]
18. Andreasson JOL, Milic B, Chen GY, Guydosh NR, Hancock WO, Block SM. Examining kinesin processivity within a general gating framework. Elife. 2015; 4:e07403.
19. Rath O, Kozielski F. Kinesins and cancer. Nat Rev Cancer. 2012; 12:527–39. [PubMed: 22825217]
20. Crevel I-TC, Alonso MC, Cross RA. Monastrol stabilises an attached low-friction mode of Eg5. Curr Biol. 2004; 14:R411–2. [PubMed: 15182685]
21. Kaan HYK, Major J, Tkocz K, Kozielski F, Rosenfeld SS. Snapshots of ispinesib-induced conformational changes in the mitotic kinesin eg5. J Biol Chem. 2013; 288:18588–18598. [PubMed: 23658017]
22. DeBonis S, Skoufias DA, Lebeau L, Lopez R, Robin G, Margolis RL, Wade RH, Kozielski F. In vitro screening for inhibitors of the human mitotic kinesin Eg5 with antimitotic and antitumor activities. Mol Cancer Ther. 2004; 3:1079–90. [PubMed: 15367702]
23. Skoufias DA, DeBonis S, Saoudi Y, Lebeau L, Crevel I, Cross R, Wade RH, Hackney D, Kozielski F. S-trityl-L-cysteine is a reversible, tight binding inhibitor of the human kinesin Eg5 that specifically blocks mitotic progression. J Biol Chem. 2006; 281:17559–17569. [PubMed: 16507573]
24. Larson AG, Naber N, Cooke R, Pate E, Rice SE. The conserved L5 loop establishes the pre-powerstroke conformation of the Kinesin-5 motor, eg5. Biophys J. 2010; 98:2619–27. [PubMed: 20513406]
25. Kapoor TM, Mayer TU, Coughlin ML, Mitchison TJ. Probing spindle assembly mechanisms with monastrol, a small molecule inhibitor of the mitotic kinesin, Eg5. J Cell Biol. 2000; 150:975–88. [PubMed: 10973989]
26. Mayer TU, Kapoor TM, Haggarty SJ, King RW, Schreiber SL, Mitchison TJ. Small molecule inhibitor of mitotic spindle bipolarity identified in a phenotype-based screen. Science. 1999; 286:971–4. [PubMed: 10542155]
27. Luo L, Carson JD, Molnar KS, Tuske SJ, Coales SJ, Hamuro Y, Sung CM, Sudakin V, Auger KR, Dhanak D, Jackson JR, Huang PS, Tummino PJ, Copeland RA. Conformation-dependent ligand regulation of ATP hydrolysis by human KSP: Activation of basal hydrolysis and inhibition of microtubule-stimulated hydrolysis by a single, small molecule modulator. J Am Chem Soc. 2008; 130:7584–7591. [PubMed: 18491908]
28. Woessner R, Tunquist B, Lemieux C, Chlipala E, Jackinsky S, Dewolf W, Voegtli W, Cox A, Rana S, Lee P, Walker D. ARRY-520, a novel KSP inhibitor with potent activity in hematological and taxane-resistant tumor models. Anticancer Res. 2009; 29:4373–4380. [PubMed: 20032381]
29. Wakui H, Yamamoto N, Kitazono S, Mizugaki H, Nakamichi S, Fujiwara Y, Nokihara H, Yamada Y, Suzuki K, Kanda H, Akinaga S, Tamura T. A phase 1 and dose-finding study of LY2523355 (litronesib), an Eg5 inhibitor, in Japanese patients with advanced solid tumors. Cancer Chemother Pharmacol. 2014; 74:15–23. [PubMed: 24752449]
30. Nakai R, Iida SI, Takahashi T, Tsujita T, Okamoto S, Takada C, Akasaka K, Ichikawa S, Ishida H, Kusaka H, Akinaga S, Murakata C, Honda S, Nitta M, Saya H, Yamashita Y. K858, a novel inhibitor of mitotic kinesin Eg5 and antitumor agent, induces cell death in cancer cells. Cancer Res. 2009; 69:3901–3909. [PubMed: 19351824]
31. Rickert KW, Schaber M, Torrent M, Neilson LA, Tasber ES, Garbaccio R, Coleman PJ, Harvey D, Zhang Y, Yang Y, Marshall G, Lee L, Walsh ES, Hamilton K, Buser CA. Discovery and biochemical characterization of selective ATP competitive inhibitors of the human mitotic kinesin KSP. Arch Biochem Biophys. 2008; 469:220–231. [PubMed: 17999913]
32. Groen AC, Needleman D, Brangwynne C, Gradinaru C, Fowler B, Mazitschek R, Mitchison TJ. A novel small-molecule inhibitor reveals a possible role of kinesin-5 in anastral spindle-pole assembly. J Cell Sci. 2008; 121:2293–300. [PubMed: 18559893]
33. Luo L, Parrish CA, Nevins N, McNulty DE, Chaudhari AM, Carson JD, Sudakin V, Shaw AN, Lehr R, Zhao H, Sweitzer S, Lad L, Wood KW, Sakowicz R, Annan RS, Huang PS, Jackson JR,

Dhanak D, Copeland RA, Auger KR. ATP-competitive inhibitors of the mitotic kinesin KSP that function via an allosteric mechanism. Nat Chem Biol. 2007; 3:722–6. [PubMed: 17922005]

34. Parrish CA, Adams ND, Auger KR, Burgess JL, Carson JD, Chaudhari AM, Copeland RA, Diamond MA, Donatelli CA, Duffy KJ, Faucette LF, Finer JT, Huffman WF, Hugger ED, Jackson JR, Knight SD, Luo L, Moore ML, Newlander KA, Ridgers LH, Sakowicz R, Shaw AN, Sung CMM, Sutton D, Wood KW, Zhang SY, Zimmerman MN, Dhanak D. Novel ATP-competitive kinesin spindle protein inhibitors. J Med Chem. 2007; 50:4939–4952. [PubMed: 17725339]
35. Yokoyama H, Sawada JI, Katoh S, Matsuno K, Ogo N, Ishikawa Y, Hashimoto H, Fujii S, Asai A. Structural basis of new allosteric inhibition in kinesin spindle protein eg5. ACS Chem Biol. 2015; 10:1128–1136. [PubMed: 25622007]
36. Chattopadhyay S, Stewart AL, Mukherjee S, Huang C, Hartwell KA, Miller PG, Subramanian R, Carmody LC, Yusuf RZ, Sykes DB, Paulk J, Vetere A, Vallet S, Santo L, Cirstea DD, Hideshima T, Dancik V, Majireck MM, Hussain MM, Singh S, Quiroz R, Iaconelli J, Karmacharya R, Tolliday NJ, Clemons PA, Moore MS, Stern AM, Shamji AF, Ebert BL, Golub TR, Raje NS, Scadden DT, Schreiber SL. Niche-Based screening in multiple myeloma identifies a kinesin-5 inhibitor with improved selectivity over hematopoietic progenitors. Cell Rep. 2015; 10:755–770.
37. Tao L, Mogilner A, Civelekoglu-Scholey G, Wollman R, Evans J, Stahlberg H, Scholey JM. A Homotetrameric Kinesin-5, KLP61F, Bundles Microtubules and Antagonizes Ncd in Motility Assays. Curr Biol. 2006; 16:2293–2302. [PubMed: 17141610]
38. Myers KA, Baas PW. Kinesin-5 regulates the growth of the axon by acting as a brake on its microtubule array. J Cell Biol. 2007; 178:1081–91. [PubMed: 17846176]
39. Cochran JC, Sontag CA, Maliga Z, Kapoor TM, Correia JJ, Gilbert SP. Mechanistic analysis of the mitotic kinesin Eg5. J Biol Chem. 2004; 279:38861–38870. [PubMed: 15247293]
40. Chen GY, Arginteanu DFJ, Hancock WO. Processivity of the Kinesin-2 KIF3A Results From Rear-Head Gating and Not Front-Head Gating. J Biol Chem. 2015; 290:10274–10294. [PubMed: 25657001]
41. Gayek AS, Ohi R. Kinetochore-microtubule stability governs the metaphase requirement for Eg5. Mol Biol Cell. 2014; 25:2051–2060. [PubMed: 24807901]
42. Sheth PR, Shipps GW, Seghezzi W, Smith CK, Chuang CC, Sanden D, Basso AD, Vilenchik L, Gray K, Annis DA, Nickbarg E, Ma Y, Lahue B, Herbst R, Le HV. Novel benzimidazole inhibitors bind to a unique site in the kinesin spindle protein motor domain. Biochemistry. 2010; 49:8350–8358. [PubMed: 20718440]
43. Ulaganathan V, Talapatra SK, Rath O, Pannifer A, Hackney DD, Kozielski F. Structural insights into a unique inhibitor binding pocket in kinesin spindle protein. J Am Chem Soc. 2013; 135:2263–2272. [PubMed: 23305346]
44. Shang Z, Zhou K, Xu C, Csencsits R, Cochran JC, Sindelar CV. High-resolution structures of kinesin on microtubules provide a basis for nucleotide-gated force-generation. Elife. 2014; 3:e04686. [PubMed: 25415053]
45. Muretta JM, Behnke-Parks WM, Major J, Petersen KJ, Goulet A, Moores CA, Thomas DD, Rosenfeld SS. Loop L5 assumes three distinct orientations during the ATPase cycle of the mitotic kinesin Eg5: A transient and time-resolved fluorescence study. J Biol Chem. 2013; 288:34839–34849. [PubMed: 24145034]
46. Goulet A, Major J, Jun Y, Gross SP, Rosenfeld SS, Moores CA. Comprehensive structural model of the mechanochemical cycle of a mitotic motor highlights molecular adaptations in the kinesin family. Proc Natl Acad Sci. 2014; 111:1837–42. [PubMed: 24449904]
47. Bakhoum SF, Genovese G, Compton DA. Deviant Kinetochore Microtubule Dynamics Underlie Chromosomal Instability. Curr Biol. 2009; 19:1937–1942. [PubMed: 19879145]
48. Sturgill EG, Norris SR, Guo Y, Ohi R. Kinesin-5 inhibitor resistance is driven by kinesin-12. J Cell Biol. 2016; 213 jcb.201507036.
49. Vladimirou E, Mchedlishvili N, Gasic I, Armond J, Samora C, Meraldi P, McAinsh A. Nonautonomous Movement of Chromosomes in Mitosis. Dev Cell. 2013; 27:411–424.

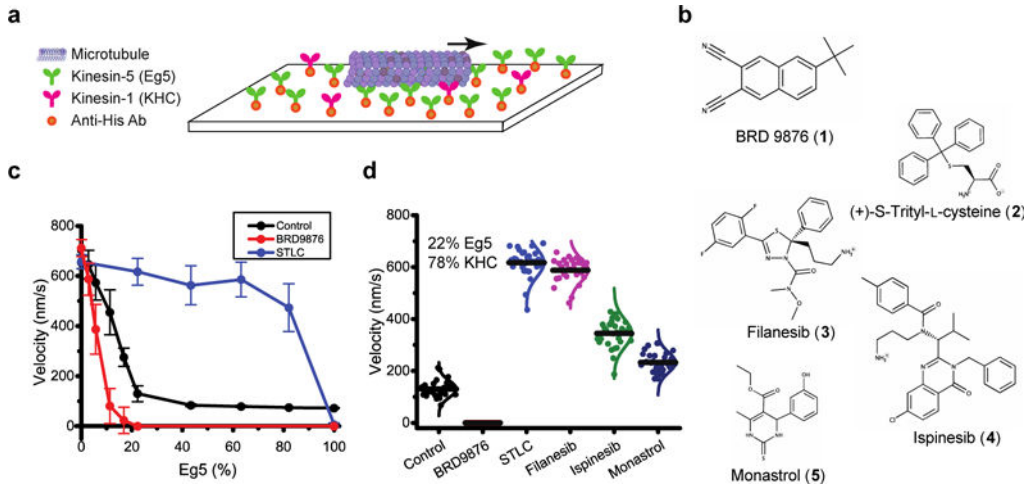


**Figure 1. Mixed-motor gliding assays reveal mechanical performance of Eg5**

(**a**) Diagram of mixed-motor gliding assays. Varying ratios of KHC and Eg5 motors were bound to a coverslip surface, maintaining a constant total motor density. (**b**) Structures of the Eg5 inhibitors used in this study. Inhibitors were present at 100 μM, which is at least an order of magnitude greater than the reported $IC_{50}$ values[23,25,27,28,36]. (**c**) Gliding velocity versus fraction of Eg5 on the surface. In the control group (black, mean ± s.d.), 22% surface coverage of Eg5 was sufficient to reduce the gliding velocity to the Eg5 speed. In the presence of 100 μM STLC (blue, mean ± s.d.), velocities at low Eg5 fractions were elevated. In contrast, BRD9876 (red, mean ± s.d.) resulted in slowed gliding, even at low Eg5 levels. (**d**) To compare different modes of inhibition, gliding velocities at 22% Eg5 were plotted for all drugs tested (see Figure S2 for full dataset). Based on their effects on Eg5 mechanical performance, these inhibitors were classified as either L5 inhibitors or Rigor inhibitors (Table 1).

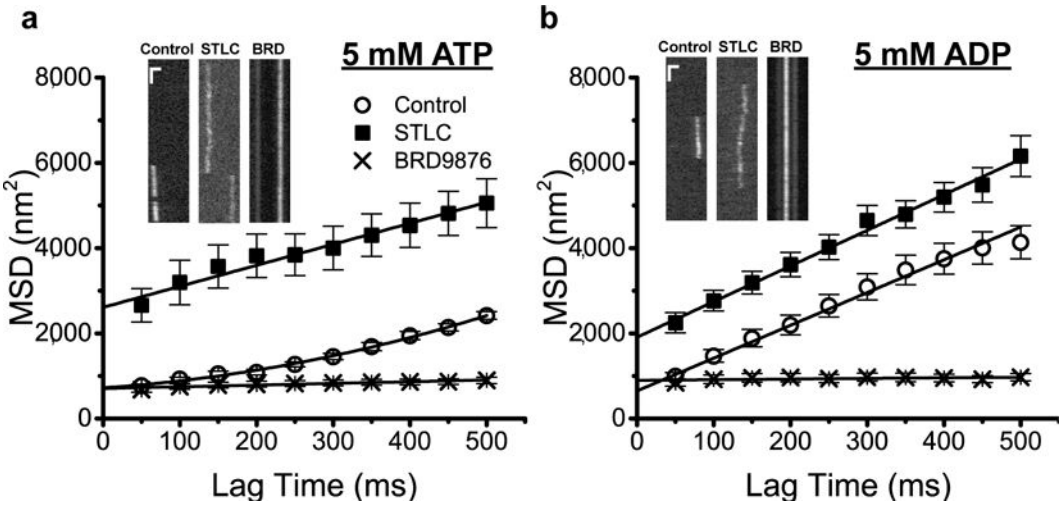


**Figure 2. Drugs produce contrasting effects on Eg5 diffusion**

Single-molecule diffusion of $QD_{655}$-labeled Eg5 along surface-immobilized MTs was measured in 5 mM ATP (**a**) or 5 mM ADP (**b**) (N = 18 – 40 events). **(a)** In the absence of drug (control; open circles) the motor walked at $v = 66 \pm 26$ nm/s and had a small diffusion coefficient ($D = 594 \pm 167$ nm$^2$/s). In saturating STLC (solid squares), the diffusive behavior was enhanced ($D = 2{,}467 \pm 161$ nm$^2$/s) while the velocity dropped to 0 nm/s. In contrast, the BRD9876-inhibited motor (BRD, crosses) bound tightly to the MT with negligible diffusion ($D = 200 \pm 25$ nm$^2$/s) and no directed motion. (**b**) In ADP, Eg5 in the absence of inhibitors (control) diffused at $D = 3{,}845 \pm 119$ nm$^2$/s, and STLC treatment slightly enhanced the diffusion ($D = 4{,}182 \pm 116$ nm$^2$/s), whereas BRD9876 treatment abolished diffusion in ADP ($D = 75 \pm 37$ nm$^2$/s), consistent with STLC and BRD9876 generating contrasting modes of inhibition. In STLC, higher motor concentrations were required to achieve a sufficient number of binding events, which resulted in greater experimental noise and a larger y-intercept in the MSD plot for STLC ($\sigma^2 = 2{,}609 \pm 95$ nm$^2$ in ATP and $1{,}908 \pm 60$ nm$^2$ in ADP) compared with the control ($\sigma^2 = 720 \pm 31$ nm$^2$ in ATP and $649 \pm 43$ nm$^2$ in ADP) and the BRD group ($\sigma^2 = 704 \pm 15$ nm$^2$ in ATP and $895 \pm 24$ nm$^2$ in ADP). **Insets:** Representative kymographs under varying conditions with scale bars of 1 μm and 1 s.

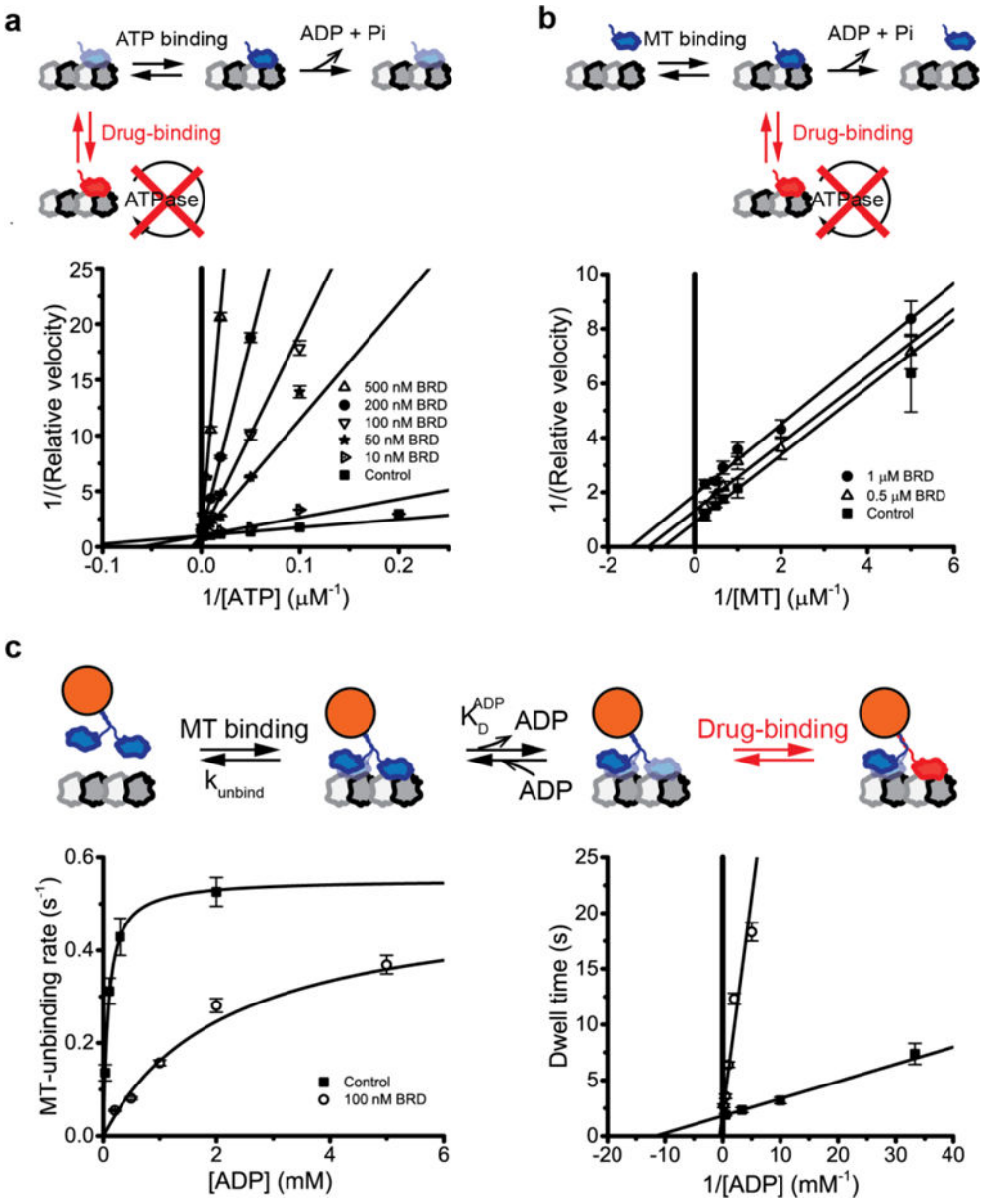


**Figure 3. Mechanism of Eg5 inhibition by BRD9876**

(**a**) ATP-dependence of monomeric Eg5 ATPase activity at 4 μM MT and varying BRD9876 concentrations. Rates were normalized to the ATPase activity at 3 mM ATP (mean ± s.d., N = 5 for each point). Increasing drug concentrations resulted in increasing $K_M$ (x-intercept) and similar $V_{max}$ (y-intercept), consistent with BRD9876 acting as an ATP-competitive inhibitor with a $K_M^{ATP}$ of 7.6 ± 0.8 μM ATP, a $K_I$ of 3.8 ± 1.5 nM BRD9876, and an $IC_{50}$ of 1.3 μM BRD9876 (Figure S4). (**b**) MT-dependence of monomeric Eg5 ATPase activity at 3 mM ATP and varying concentrations of BRD9876. The decrease in $V_{max}$ (y-intercept) and increase in $K_M$ (x-intercept) with increasing BRD9876 concentrations are consistent with MT-uncompetitive inhibition, with a $K_D^{MT}$ of 1.4 ± 0.2 μM MT. (**c**) Left: Single-molecule binding durations of dimeric Eg5 at varying ADP concentrations, measured by TIRF imaging of Qdot655-labeled motors. Control data were fit to a 3-state model with $k_{unbind}$ of

$0.55 \pm 0.02\ s^{-1}$ and $K_D^{ADP}$ of 86 ± 7 μM ADP (control, square). In the presence of 100 nM BRD9876 (open circles), off-rates were reduced, consistent with the drug trapping the motor in the MT-bound apo-state. Data were fit to a 3-state model with $k_{unbind} = 0.52 \pm 0.18\ s^{-1}$ and $K_D^{apparent} = 2.2 \pm 1.1$ mM ADP, giving $K_I = 4.1$ nM BRD9876. Right: Data plotted as Lineweaver-Burk to emphasize similar $k_{unbind}$ (y-intercept) and different apparent $K_D^{ADP}$ (x-intercept), indicating that BRD9876 acts as an ADP-competitive inhibitor.

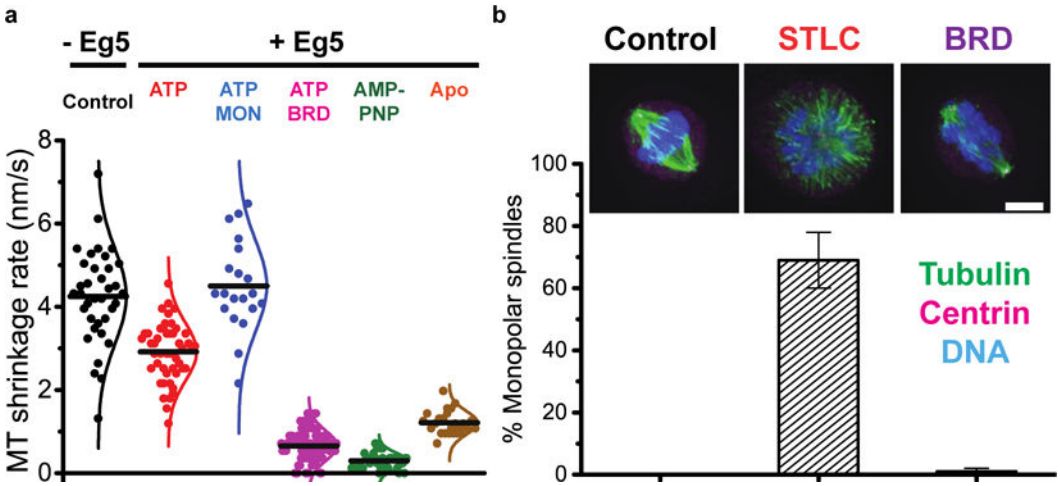


**Figure 4. Effects of Eg5 inhibitors on microtubule stability and spindle integrity**

(**a**) Effects of inhibitors on MT depolymerization following taxol washout. Cy5-labeled, taxol-stabilized MTs were bound to coverslips using a kinesin-1 rigor mutant, and taxol was washed out to induce MT depolymerization. For ATP and MON+ATP, Eg5 was presented at 40 nM, whereas for the strong-binding species BRD, AMPPNP, and Apo, only 5 nM Eg5 was used, emphasizing the potency of Eg5 in stabilizing MT under these conditions. All samples included 1 vol% DMSO. All data are shown (points) along with the mean (line) and fit to a normal distribution (curve). (**b**) Spindle collapse assays in the presence of varying inhibitors. Representative images of RPE-1 cells are shown, immunostained for tubulin (green), centrin (magenta), and DNA (blue). Scale bar: 5 μm. Quantification of spindle integrity. In the control group (no Eg5 inhibitor), the spindle retained its bipolar geometry and no monopolar spindles were observed (N = 89). In the presence of the L5 inhibitor STLC, 69 ± 9% of spindles collapsed to monopole phenotype (mean ± s.d., N = 94). In contrast, in the presence of the rigor inhibitor BRD9876, 1 ± 1% spindles were monopolar (mean ± s.d., N = 81). Eg5 localization under different conditions is shown in Figure S6.

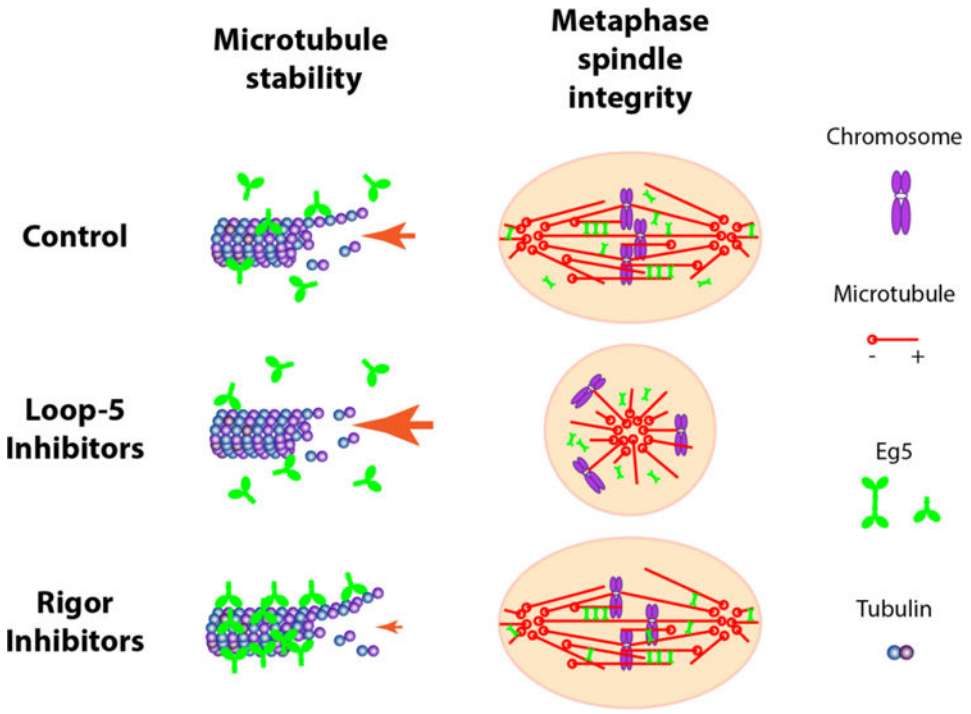


**Figure 5. Different mechanisms of Eg5 inhibition**

The biological impacts of diverse Eg5 inhibitors on MT stability and the spindle integrity are presented graphically. Treatment with L5 inhibitors induces a weak-binding state in Eg5, knocking Eg5 off the microtubules and reducing its effective concentration. This eliminates the Eg5 microtubule polymerase and stabilization activities, and additionally causes metaphase spindle collapse. In contrast, rigor inhibitors induce a strong-binding state in Eg5, which enhances microtubule stabilization and crosslinks metaphase spindles, which maintains spindle bipolarity in already-formed spindles.

## Table 1

List of ligands and the corresponding mechanical types.

| Ligand | Mechanical response[a] | Unloaded MT off-rate, ($k_{off}^0$, $s^{-1}$) | Detachment Force ($F_c$, pN) | Class |
|---|---|---|---|---|
| **Control** | – | 0.35 | 17 | – |
| **Monastrol** | Weak-binding | 0.92 | 27 | Less potent L5 |
| **Ispinesib** | Weak-binding | 1.50 | 18 | Less potent L5 |
| **STLC** | Weak-binding | 1.45 | 0.6 | Potent L5 |
| **Filanesib (ARRY-520)** | Weak-binding | 1.74 | 2.4 | Potent L5 |
| **BRD9876** | Strong-binding | 0.01[b] | 14 | Rigor |

[a] Mechanical classification according to Figure 1, 2, and Figure S1.

[b] MT-unbinding rate in BRD9876 was estimated by its $IC_{50}$ in 3 mM ATP.